

Configuration of membrane-bound proteins by x-ray reflectivity

Chiu-Hao Chen,¹ Šárka Málková,¹ Wonhwa Cho,² and Mark L. Schlossman^{1,a)}

¹*Department of Physics, University of Illinois at Chicago, Chicago, Illinois 60607, USA*

²*Department of Chemistry, University of Illinois at Chicago, Chicago, Illinois 60607, USA*

(Received 15 October 2010; accepted 21 November 2010; published online 30 November 2011)

In this presentation we review our recent work using x-ray reflectivity to determine the configuration of membrane-bound proteins. The reflectivity data is analyzed in terms of the known crystallographic structure of proteins and a slab model representing the lipid layer to yield an electron density profile of the lipid/protein system. Our recent modified analysis methodology for the lipid/protein system is concisely described in this report. In addition, some results of the configuration of the membrane-bound proteins cPLA₂ α -C2, p40^{phox}-PX, and PKC α -C2 are highlighted. © 2011 American Institute of Physics. [doi:10.1063/1.3661985]

I. INTRODUCTION

Peripheral membrane proteins that are important for cell signaling and vesicle trafficking are specifically targeted to cell membranes. Because the function and regulation of a majority of peripheral proteins depend upon their interactions with membranes, it is essential to determine the structural arrangement of peripheral proteins and membrane targeting domains at the membrane, including their membrane-bound orientation and depth of penetration. These structural parameters have been studied by mutational studies, electron spin resonance (EPR), MD simulations, and x-ray reflectivity measurements.^{1–6}

A common method of analysis that has been applied previously to reflectivity data measured from proteins bound to lipid monolayers relies upon modeling the electron density profile as three distinct slabs, each of uniform density, sandwiched between a bulk aqueous buffer and bulk air.^{7–9} The first two slabs represent the average electron density in the tailgroup (acyl group) and headgroup regions of the lipid monolayer and the third slab describes the protein. Two problems arise as a result of treating the protein as an additional slab of uniform electron density. The first is that this model does not provide direct insight into the bound configuration of the protein, that is, its angular orientation and depth of penetration of the protein into the region of the lipid monolayer. The second is that information is lost by modeling the protein as rectangular and this lost information may lead to an incorrect interpretation of the reflectivity.

We used the known crystallographic structure of the protein and a two-slab model representation of the lipid monolayer in order to quantitatively extract the orientation and penetration of the protein into the monolayer. Initially, the commercial crystallography software CERUS was used to compute the protein's electron density profile.^{2,3} Recently, we wrote custom software that uses the protein's Protein Data Bank (PDB) file as input.¹ Current evidence indicates that the proteins that we have studied do not undergo significant conformational rearrangement upon interacting with the

lipid layer.^{10–13} As a result, it is sensible to model these proteins with their crystallographic structure. However, it should be emphasized that this analysis methodology is not limited to treating reflectivity data from proteins that do not change their conformation upon binding. For example, the crystal structure itself may indicate a plausible rearrangement of the protein structure upon binding, or molecular dynamics simulations or other observations may suggest such rearrangements. These rearrangements can be incorporated into the current methodology by modifying the input PDB file. This analysis technique will then allow the proposed rearrangements to be tested against x-ray reflectivity data.

In Sec. II the data analysis method is outlined. Application of this method to x-ray reflectivity from PKC α -C2 domains bound to mixed SOPC(1-stearoyl-2-oleoyl-sn-glycero-3-phosphocholine)/SOPS(1-stearoyl-2-oleoyl-sn-glycero-3-phosphoserine) (7:3 molar ratio) lipid monolayers indicates that the domain is bound in a perpendicular orientation with a well-defined penetration depth.¹ Under the assumption that the protein conformation has not changed upon binding, the determined orientation and penetration of the protein predicts the location of amino acid residues of the protein with respect to average positions of chemical moieties on the lipids, though it should be emphasized that the locations of the residues are not determined directly. We have shown that these locations compare favorably with the results of biochemical mutational studies.¹ We also discuss briefly our earlier studies of the bound configuration of cPLA₂ α -C2 domains² bound to SOPC lipid molecules and p40^{phox}-PX domains³ interacting with DPPTdIns(3)P. These studies of monolayer-bound configurations of proteins provide insight into the contributions of electrostatic and hydrophobic interactions, as well as the role of entropy in the binding mechanism.

II. EXPERIMENTAL METHODS

A. X-ray reflectivity

X-ray reflectivity experiments were carried out at beamline X19C at the National Synchrotron Light Source (Brookhaven National Laboratory, Upton, NY) with a liquid surface scattering instrument described in detail elsewhere.¹⁴

^{a)}Author to whom correspondence should be addressed. Electronic mail: schlossm@uic.edu.

Reflectivity is measured as a function of the wave vector transfer, Q_z , by varying the incident angle, α , and measuring the intensity of scattered x-rays at the reflected angle α . The wave vector transfer of the reflected x-rays, Q , is solely in the z -direction normal to the buffer surface with $Q_z = (4\pi/\lambda) \sin \alpha$, where $\lambda = 1.54 \pm 0.003$ Å is the x-ray wavelength; therefore, x-ray reflectivity probes variations in electron density as a function of depth into the surface. Deviations of the measured reflectivity, $R(Q_z)$, from the Fresnel reflectivity calculated for an ideal, smooth and flat interface, $R_F(Q_z)$, reveal the presence of interfacial structure as a function of surface depth.

III. DATA ANALYSIS

A. Electron density profile of a protein in a box at an arbitrary orientation

Here, we present a general method that underlies a computationally fast calculation of the electron density profile for a protein bound to a lipid monolayer supported on water. Additional details can be found in Ref. 1. The protein is rotated as a rigid body by two of the Euler angles, i.e., θ and φ . The angle θ measures the angle between the protein's z' -axis and the surface normal, whereas the angle φ is an azimuthal rotation about the direction of the z' -axis. Rotation of the protein by the angle ψ , which corresponds to an azimuthal rotation within the plane of the surface, does not change the electron density profiles of the protein along the surface normal. For each orientation, the smallest possible rectangular box with sides parallel to the x -, y -, and z -axes is constructed for the protein.

The electron density profile along the z_p -axis of a box was computed by partitioning the box into a cubic grid of cell dimension ~ 0.5 Å. We assume that the electrons associated with each atom are spread uniformly and continuously throughout the van der Waals spherical volume of that atom. Electrons from an atom are assigned to a given cell if the van der Waals sphere of that atom overlaps a pre-chosen corner of the cell (where the set of pre-chosen corners form a rectangular, though nearly square, lattice). The number of assigned electrons is determined by the ratio of the cell volume to the atomic volume. The total number of electrons in a given cell n_{cell} is determined by the sum of overall atoms k whose van der Waals volume V_k overlaps the pre-chosen corner of that cell,

$$n_{cell} = \sum_k \frac{V_{cell}}{V_k} n_k, \quad (1)$$

where n_k is the number of electrons in atom k and V_{cell} is a cell volume. The total number of protein electrons in a single layer of cells at height z_p is computed by summing the electrons in all cells at a given height z_p . The electron density $\rho_{ep}(z_p)$ (at height z_p in the empty box with protein, see Fig. 1(a)) is then computed by dividing this total by the volume of a grid layer. In a buffer box, otherwise empty cells are assigned the value of the buffer's electron density. When the number of electrons from the buffer at height z_p is added to the number of electrons from the protein at the same

height, the electron density $\rho_{bp}(z_p)$ (of the buffer box with protein, see Fig. 1(b)) can be calculated. The connection of z_p and z can be related via $z = z_p + d_p$, where the displacement of the protein d_p is the distance from the surface.

B. Electron density profile of the whole system

The electron density profile along the z -axis for the lipid monolayer with bound proteins (Fig. 1(c)) is constructed by combining the electron densities $\rho_{ep}(z_p)$ and $\rho_{bp}(z_p)$ with the electron density of the lipid tailgroup and headgroup (characterized by L_{tail} , ρ_{tail} , L_{head} , and ρ_{head}). The electron density in the region of the lipid monolayer on the interface is given by,

$$\rho_i(z) = COV \times \rho_{ep}(z_p) + \rho_{tail} \quad \text{for} \quad -L_{tail} \leq z < 0, \quad (2)$$

$$\rho_i(z) = COV \times \rho_{ep}(z_p) + \rho_{head} \quad \text{for} \quad -(L_{tail} + L_{head}) \leq z < -L_{tail}. \quad (3)$$

The protein coverage, COV , is the fraction of surface area occupied by protein-filled boxes. In the buffer region below the lipid monolayer:

$$\rho_i(z) = COV \times \rho_{bp}(z_p) + (1 - COV)\rho_{buffer} \quad \text{for} \quad -L_{protein} + d_p \leq z < -(L_{tail} + L_{head}), \quad (4)$$

where $L_{protein}$ is the height of the protein box for a given orientation. In the region of bulk buffer for $z < -L_{protein} + d_p$ the electron density is given by ρ_{buffer} .

Capillary wave thermal fluctuations of the water surface smear the average electron density $\rho(z)$. This effect is calculated by convoluting the intrinsic profile $\rho_i(z)$ with a Gaussian function of width σ , the capillary roughness, by using

$$\rho(z) = \int_{-\infty}^{\infty} G(z - \zeta) \rho_i(\zeta) d\zeta \quad (5)$$

$$G(z) = \frac{1}{\sqrt{2\pi}\sigma^2} \exp\left(-\frac{z^2}{2\sigma^2}\right)$$

The continuous electron density profile $\rho(z)$ of the interface is then sliced into M layers of thickness 1 Å for the purpose of calculating the reflectivity using the Parratt formalism.

C. Reflectivity fitting procedure

A total of eight fitting parameters, i.e., θ , φ , d_p , COV , L_{tail} , ρ_{tail} , L_{head} , and ρ_{head} , are used to produce an electron density profile for the lipid-protein system. In the fitting algorithm, the x-ray reflectivity data is fit by non-linear least square fitting using six of these parameters (d_p , COV , L_{tail} , ρ_{tail} , L_{head} , and ρ_{head}) for a given orientation. The six-parameter fitting is then repeated by stepping through a large range of orientations in θ - φ space. The density of orientations is varied in order to precisely locate the best-fit value in θ - φ space. The goodness of fit parameter χ^2 is computed for each eight-parameter set.

IV. RESULTS

This data analysis method was applied to determine the membrane-bound configuration of PKC α -C2 on a mixed

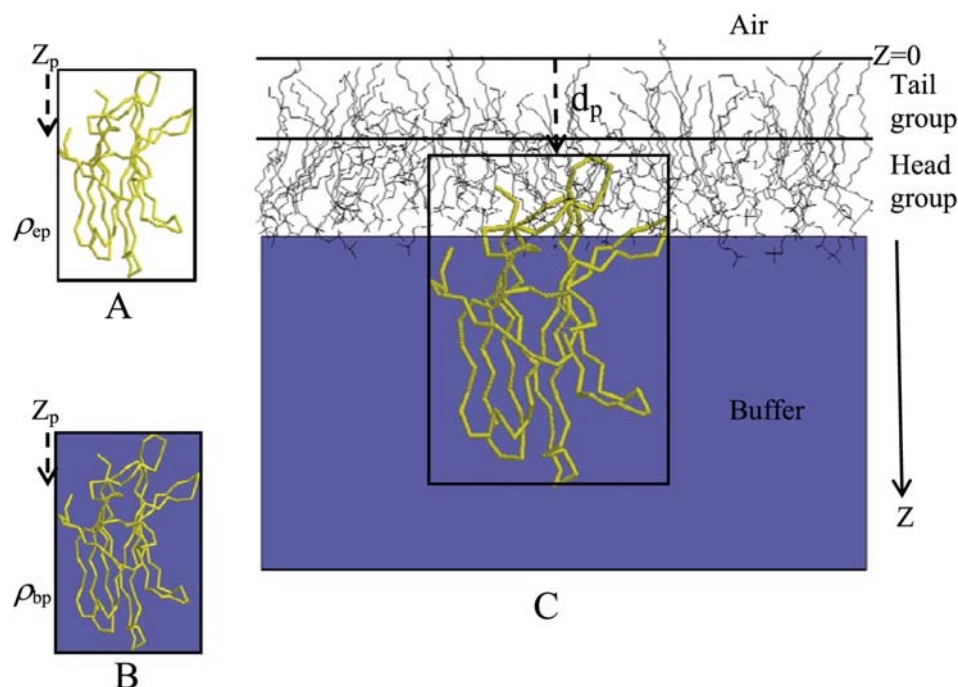


FIG. 1. (Color online) Protein structure in (a) an empty box and (b) a buffer box; (c) the fitting docking model of the lipid monolayer-protein.

lipid monolayer (7:3 SOPC:SOPS) supported on the surface of a buffered aqueous solution that contains PKC α -C2 domain (see Fig. 1).¹ The orientation of the monolayer-bound protein is characterized by $\theta = 35^\circ \pm 10^\circ$ and $\varphi = 210^\circ \pm 30^\circ$. In this configuration the protein penetrates a distance of 7.5 ± 2 Å into the lipid headgroup. Our analysis shows that the PKC α -C2 domain does not insert into the hydrophobic region of the lipid layer and that the calcium binding loops CBL1 and CBL2 penetrate into the lipid headgroup while CBL3 is located adjacent to the headgroup. Residues that penetrate into the headgroup region are predominantly polar or charged, which indicates that electrostatic interactions significantly contribute to the free energy of PKC α -C2 bound to lipid monolayers.

In earlier studies that used a somewhat restricted version of the current analysis methodology, the configuration of p40^{phox}-PX domain bound to SOPC/SOPS/PtdIns(3)P(1,2-dipalmitoylphosphatidylinositol 3-phosphate) monolayers requires the out of plane migration of PtdIns(3)P.³ This is an important clue to the interaction of phosphatidylinositols with membrane proteins. In another earlier study, the bound configuration of cPLA2 α -C2 domain adsorbed onto Langmuir monolayers of SOPC indicated that both electrostatic and hydrophobic interactions are relevant for the mechanism of binding.² Electrostatic interactions are relevant because analysis of the reflectivity indicated that Ca²⁺ ions that are bound to the C2 domain are situated near the negatively charged lipid phosphate groups in the bound configuration. Hydrophobic interactions are relevant because hydrophobic residues L39 and V97, located in the calcium-binding loops, penetrate into the region of the lipid tailgroup. Importantly, calculation of the electron density profiles of the total number of electrons per lipid suggested that at least five water molecules leave the lipid headgroup upon protein binding, thereby providing an entropic driver to the binding process.

V. CONCLUSION

The analysis methodology for x-ray reflectivity described in this paper allows for quantitative characterization of the configuration of membrane-bound proteins, which provides an essential understanding of the interaction between lipid molecules and proteins in a molecular scale. This characterization provides insight into the interactions that control protein binding to biomembranes, as well as their catalytic function.

ACKNOWLEDGMENTS

This work was supported by National Science Foundation (NSF) grants (Nos. CHE0315691 and CHE0615929 to M.L.S.) and National Institutes of Health (NIH) grants (GM68849 and GM76581 to W.C.). M.L.S. thanks Dr. Aleksey Tikhonov for help with the X19C beamline at National Synchrotron Light Source (NSLS) (Brookhaven National Laboratory), which was partially supported by ChemMat-CARS (supported by NSF-CHE, NSF-DMR, and the Department of Energy (DOE)). The Brookhaven National Laboratory and the NSLS are supported by DOE. C.H.C thanks Dr. Manoj Athavale and Binyang Hou for help with the analysis and Dr. Shekhar Garde with help in the computational algorithm of the most recent analysis code. We thank Diana Murray for modifying the PDB file to include the additional residues from the purification protocol.

¹C. H. Chen, S. Malkova, S. V. Pingali, F. Long, S. Garde, W. Cho, and M. L. Schlossman, *Biophys. J.* **97**, 2794 (2009).

²S. Malkova, F. Long, R. V. Stahelin, S. V. Pingali, D. Murray, W. Cho, and M. L. Schlossman, *Biophys. J.* **89**, 1861 (2005).

³S. Malkova, R. V. Stahelin, S. V. Pingali, W. Cho, and M. L. Schlossman, *Biochemistry* **45**, 13566 (2006).

⁴N. J. Malmberg and J. J. Falke, *Annu. Rev. Biophys. Biomol. Struct.* **34**, 71 (2005).

- ⁵D. Manna, N. Bhardwaj, M. S. Vora, R. V. Stahelin, H. Lu, and W. Cho, *J. Biol. Chem.* **283**, 26047 (2008).
- ⁶M. Medkova and W. Cho, *J. Biol. Chem.* **273**, 17544 (1998).
- ⁷D. Gidalevitz, Z. Huang, and S. A. Rice, *Proc. Natl. Acad. Sci. U.S.A.* **96**, 2608 (1999).
- ⁸D. Gidalevitz, Y. Ishitsuka, A. S. Muresan, O. Konovalov, A. J. Waring, R. I. Lehrer, and K. Y. Lee, *Proc. Natl. Acad. Sci. U.S.A.* **100**, 6302 (2003).
- ⁹K. Y. Lee, J. Majewski, T. L. Kuhl, P. B. Howes, K. Kjaer, M. M. Lipp, A. J. Waring, J. A. Zasadzinski, and G. S. Smith, *Biophys. J.* **81**, 572 (2001).
- ¹⁰N. J. Malmberg, D. R. Van Buskirk, and J. J. Falke, *Biochemistry* **42**, 13227 (2003).
- ¹¹O. Perisic, S. Fong, D. E. Lynch, M. Bycroft, and R. L. Williams, *J. Biol. Chem.* **273**, 1596 (1998).
- ¹²N. Verdaguer, S. Corbalan-Garcia, W. F. Ochoa, I. Fita, and J. C. Gomez-Fernandez, *Embo J* **18**, 6329 (1999).
- ¹³G. Y. Xu, T. McDonagh, H. A. Yu, E. A. Nalefski, J. D. Clark, and D. A. Cumming, *J. Mol. Biol.* **280**, 485 (1998).
- ¹⁴M. L. Schlossman, D. Synal, Y. Guan, M. Meron, G. Shea-McCarthy, Z. Huang, A. Acero, S. M. Williams, S. A. Rice, and P. J. Viccaro, *Rev. Sci. Instrum.* **68**, 4372 (1997).